Flanges classified under the International Electrotechnical Commission, British RCSC, American Armed Services, and American EIA nomenclature systems are listed in Table I. The numbers tabulated along with the publications referenced will serve to identify the majority of flanges currently in use. It is unfortunate, but true, that flanges fitting the same waveguide size, but belonging to different nomenclature systems, may not mate. In case of doubt, the publications listed below should be consulted for precise mechanical details.

The International Electrotechnical Commission system [1] comprises numbers "154 IEC-( )" containing, in sequence, the following information: 1) "*P*" for pressurizable, "*C*" for pressurizable choke, or "*U*" for unpressurizable; 2) *A*, *B*, *C*, *D*, *E*, or *F* to denote the appropriate mechanical features; and 3) the number of the IEC waveguide with which the flange is used.

The British RCSC system [2] comprises catalog numbers "5985-99-( )" which contain no information concerning the flange type or construction.

The Armed Services preferred flanges are those "UG-( )/*U*" flanges recommended for use in new equipment. The numbers contain no information on flange type or construction. Preferred flanges and other RF equipment is listed in a handbook [3].

The EIA system [4] comprises numbers which contain, in sequence, the following information: 1) "*C*" for connector, 2) "*M*" for miniature contact or "*P*" for pressurizable contact; 3) "*R*" for rectangular waveguide; 4) number of the EIA waveguide with which the flange is used.

It is encouraging to note that some groups favor a reduction in the total number of designations; Germany's DIN group has begun to adopt the IEC nomenclature system [5]. Convenience dictates that such a change is not possible for all presently-used systems. It is suggested, however, that all specifications should carry the IEC designation in addition to any other system used For example: "The instrument uses RG-39/U (similar to and will mate with 154 IEC-UBR 100) flanges."

M. Michael Brady
Norwegian Defence Research Est.
Kjeller, Norway

References

[1] International Electrotechnical Commissions Flanges for waveguides pt 1: general requirement, and measuring methods, Publication 154-1 (1964); Pt 2: relevant specifications for flanges for ordinary rectangular waveguides, Publication 154-2 (1965), IEC, Geneva. (Available from national committees or Bureau Central de la Commission Electrotechnique Internationale, I, rue de Varembe, Geneva, Switzerland.)

[2] Ministry of Defence, Defence specification DEF-5352, couplings, waveguide, Her Majesty's Stationery Office, London, England, 1958, reprinted with amendments Oct 1963. (Available from: Her Majesty's Stationery Office, York House, Kingway, London, W.C. 2, England.)

[3] Department of Defense, Military standardization handbook, RF transmission lines and fittings MIL-HDBK-216, Defense Supply Agency, Washington, D. C., Jan 4, 1962. (Available from: Naval Supply Depot, 5801 Tabor Avenue, Philadelphia, Pa. 19120, U.S.A.)

[4] Electronic Industries Association, EIA standards RS-166 (May 1962) and RS-271A (Nov 1963), EIA, N. Y. (Available from: Electronic Industries Association, Engineering Department, 11 West Forty-Second Street, New York 36, N. Y., U.S.A.)

[5] Deutsche Industrie Normen, DIN 47303, Flansche fur Rohre fur HF-Hohlleiter, DIN, Aug 1960 and Mar 1964. (Available from: Beuth-Vertrieb GmbH, Berlin 15 and Köln, Germany.)

Optimum Design of Helix Couplers with Shielding

Helix couplers have to be shielded to insure good match to coaxial cables. In our calculations the effect of the shielding has also been taken into consideration. As a result of this, the calculated dimensions of helix couplers approximate more closely the best experimentally obtained ones.

The calculation is based on simplifying assumptions. The real helix is substituted by a helically conducting cylindrical tube of infinite length and zero thickness. The effect of the dielectric materials is neglected.

In computing the coupling factor, the effect of shielding should also be taken into account. Then, as an approximation the shield itself is also regarded as a helically conducting surface. In this way three coupling factors can be calculated. The resulting coupling factor is given by [1]

$$k = k_{1,2}\sqrt{\frac{1 - k_{2,3}^2}{1 - k_{1,3}^2}} \tag{1}$$

where $k_{1,2}$ $k_{1,3}$, and $k_{2,3}$ are the coupling factors between the inner helix and coupling helix, the inner helix and shield, and the coupling helix and shield, respectively.

If the phase velocities along the helices are equal, the coupling factors are obtained as [2]

$$\left.\begin{aligned} k_{1,2} &= e^{-\beta(a_2-a_1)} \\ k_{1,3} &= e^{-\beta(a_3-a_1)} \\ k_{2,3} &= e^{-\beta(a_3-a_2)} \end{aligned}\right\} \tag{2}$$

where β is the common phase constant of propagation along coupled helices, a_1 is the mean radius of inner helix, a_2 is the mean radius of coupling helix, a_3 is the inner radius of the shield. The coupling phase constant for synchronous helices is [2]

$$\beta_c = 2\beta k. \tag{3}$$

Hence the coupling wavelength is

$$\lambda_c = \frac{2\pi}{\beta_c} = \frac{\pi}{\beta k}. \tag{4}$$

In order to completely transfer the power, the length of the coupling helix must be equal to half of the coupling wavelength λ_c.

To arrive at an optimum dimensioning of helix couplers, let us examine the relation between the coupling phase constant and the phase constant of the propagation along an uncoupled helix. This will, at the same time, give the approximate frequency dependence of the coupling phase constant, as the phase constant along a single helix is proportional to the frequency.

The inner radius of the shield can be expressed as

$$a_3 = a_2 + h \tag{5}$$

where h is the mean distance between the coupling helix and its shield.

The relation between the coupling phase constant and the single helix phase constant is obtained by substituting (1) and (2) into (3) and taking into account (5). Then we get

$$\beta_c = 2\beta e^{-\beta(a_2-a_1)}\sqrt{\frac{1 - e^{-2\beta h}}{1 - e^{-2\beta(a_2-a_1+h)}}}. \tag{6}$$

It is more advantageous to have this equation written in a dimensionless form. To this end both sides of the equation are multiplied by a_1 and the exponents are transformed with the result

$$\beta_c a_1 = 2\beta a_1 e^{-\beta a_1((a_2/a_1)-1)}\sqrt{\frac{1 - e^{-2\beta a_1(h/a_1)}}{1 - e^{-2\beta a_1((a_2/a_1)-1+(h/a_1))}}}. \tag{7}$$

Equation (7) includes two parameters; a_2/a_1 is the ratio of the mean radius of the coupling helix to that of the inner helix; h/a_1 is the ratio of the mean distance between the coupling helix and its shield to the inner-helix mean radius.

Figure 1 shows the dependence of $\beta_c a_1$ on βa_1 for different h/a_1 values, with $a_2/a_1 = 2$. The curve with $h/a_1 = \infty$ corresponds to the case when the coupling helix is not shielded. The remaining curves indicate the effect of shielding. It is to be seen from this figure that taking into account the effect of the shield a lower value is obtained for β_c; that gives a longer coupling helix as compared to that obtained when the effect of the shield is neglected. Consequently, a better agreement with the experimental results is attained if the effect of the shield is taken into account [3].

In the vicinity of the maximum the coupling phase constant has a nearly constant value over a wide band as seen in Fig. 1. Therefore, the maximum of the curve

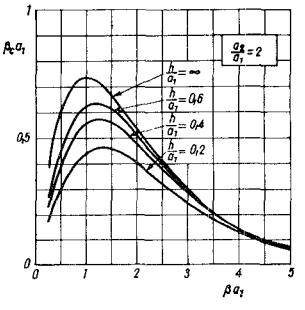

Fig. 1. Coupling phase constant as a function of the single-helix phase constant for different h/a_1 values, with $a_2/a_1 = 2$.

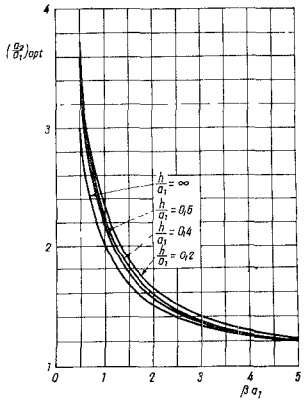

Fig. 2. Optimum a_2/a_1 ratio as a function of the single-helix phase constant for different h/a_1 values.

Manuscript received August 17, 1964; revised February 15, 1965.

$\beta_c a_1$ must be kept at the mean frequency of the operating band, when wide-band couplers are needed. In practical cases the mean frequency and the dimensions of the inner helix are given, and the value of h is determined by the characteristic impedance of the connecting cable. Thus βa_1 and h/a_1 are known, and from these values the ratio of the two radii have to be determined to get the maximum at a given value of βa_1.

In order to determine the position of the maximum, β_c must be differentiated with respect to β and the differential quotient made equal to zero. And so the equation

$$\frac{a_2}{a_1} - 1 - \frac{1}{\beta a_1} + \left(\frac{a_2}{a_1} - 1 + \frac{h}{a_1}\right) \cdot \frac{e^{-2\beta a_1((a_2/a_1)-1+(h/a_1))}}{1 - e^{-2\beta a_1((a_2/a_1)-1+(h/a_1))}} - \frac{h}{a_1} \frac{e^{-2\beta a_1(h/a_1)}}{1 - e^{-2\beta a_1(h/a_1)}} = 0 \quad (8)$$

is obtained. In the limit case, when $h/a_1 = \infty$, (8) has the simpler form

$$\frac{a_2}{a_1} - 1 - \frac{1}{\beta a_1} = 0. \quad (9)$$

This corresponds to the case when the distance of the shield to the coupling helix is infinite, that is when the coupling helix is not shielded. Consequently, the effect of the shield is given by the fourth and fifth terms at the left side of (8).

The solution of (8) cannot be given in an explicit form. Therefore, this equation has been solved numerically for several values of βa_1 and h/a_1 by successive approximations. In Fig. 2 the optimum values for the ratio of two radii a_2/a_1 obtained by solving (8) are given as a function of βa_1 for different values of h/a_1. It is apparent that, taking the effect of shielding into account, a higher value for the optimum ratio of radii is obtained than without the shield. Moreover, it is to be seen that decreasing the spacing between the coupling helix and the shield, the optimum ratio of the radii is increased.

T. Berceli
Telecommun. Research Institute
Budapest, Hungary

References

[1] Wade, G., and N. Rynn, Coupled helices for use in traveling-wave tubes, *IRE Trans. on Electron Devices*, vol ED-2, Jul 1955, pp 15–24.
[2] Cook, J. S., R. Kompfner, and C. F. Quate, Coupled helices, *Bell Sys. Tech. J.*, 1956, pp 127–178.
[3] Berceli, T., Design of helix couplers, *Acta Tech. Hungar.*, vol 31, nos. 3–4, 1960, pp 311–341.

Dispersion of Pulsed Electromagnetic Waves in a Plasma

Observations of the dispersion of electromagnetic pulses in isotropic plasmas [1] and gyrotropic plasmas [2] show that the response is distorted due to the excitation of weakly damped oscillations characteristic of the natural frequencies of the plasma. For diagnostic application, signals with a smooth frequency spectrum, such as steps or short unidirectional pulses, allow a simple correlation between the observed response and the relevant plasma parameters. In radar or communications systems, however, the dispersion of sinusoidal pulses carrying information in the pulse amplitude or in the pulse duration is important. Due to the relatively high spectral intensity near the carrier frequency, a pronounced signal distortion arises if the carrier frequency is comparable to a natural oscillation frequency of the plasma.

We have calculated the distortion of a pulsed electromagnetic wave (angular frequency ω_s) caused by a reflection from a semi-infinite uniform and isotropic plasma (angular plasma frequency ω_p), and the distortion of a pulsed wave transmitted through a plasma by convolution of the response for a short unidirectional pulse. For the reflected wave, the impulse response is [1]

$$v_r(t) = -\frac{2J_2(\omega_p t)}{t}. \quad (1)$$

Hence, for a carrier pulse of duration T_0 and amplitude V_0,

$$V_r(t) = V(t) - V(t - T_0)$$

with

$$V(t) = -2V_0 \int_0 \sin\omega_s(t-\tau)\frac{J_2(\omega_p\tau)}{\tau}d(\tau). \quad (2)$$

Computer results for three different ratios between the carrier frequency and the plasma frequency are shown in Fig. 1(a) as a function of time. For comparison with the experimental observations, a pulse duration of three cycles has been assumed. The initial response is dominated by low-frequency components of the incident carrier pulse $\omega < \omega_p$, for which the magnitude of the reflection coefficient is large ($r = -1$). The first peak is inverted with respect to the polarity of the incident wave and is progressively delayed in time for lower electron densities. The response subsequently tends to approach the steady-state condition for the assumed carrier frequency. Following the termination of the pulse, a characteristic transient ringing arises, which in time approaches the plasma frequency. The amplitude of this oscillation simply reflects the spectral intensity of the exciting signal near the plasma frequency.

A short voltage impulse set up inside an unbounded plasma at $z = 0$ gives rise to a signal at $z = d$ of the form [1]

$$v_T(t) = \delta(t - d/c_0) - \omega_p \frac{d}{c_0} \frac{J_1(\omega_p\sqrt{t^2 - (d/c_0)^2}}{\sqrt{t^2 - (d/c_0)^2}} \quad (t \geqq d/c_0). \quad (3)$$

Hence, the transmitted signal response for a carrier pulse of duration T_0 is

$$V_T(t) = V(t) - V(t - T_0)$$

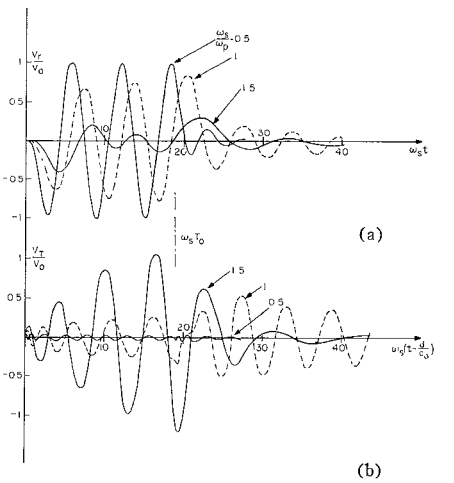

Fig. 1. Dispersion of short sinusoidal pulses in a plasma. Pulse duration 3 cycles, angular carrier frequency ω_s, amplitude V_0. (a) pulse reflected from a plasma-air interface. (b) pulse transmitted through a distance d in a plasma ($\theta = 15$).

with

$$V(t) = V_0\left\{\sin(\omega_s t - \theta) - \frac{\theta}{\omega_s/\omega_p} \int_{\omega_s\tau=\theta}^{(\omega_s t)} \sin\omega_s(t-\tau) \cdot \frac{J_1((\omega_p/\omega_s)\sqrt{(\omega_s\tau)^2 - \theta^2})}{\sqrt{(\omega_s\tau)^2 - \theta^2}} d(\omega_s\tau)\right\} \quad (\omega_s t \geqq \theta), \quad (4)$$

where $\theta = \omega_s d/c_0$.

The response shown in Fig. 1(b) for $\theta = 15$ exhibits a slow build-up of the RF oscillation in underdense plasmas ($\omega_s/\omega_p = 1.5$ and 1.10), followed by a persistent transient oscillation near the plasma frequency after termination of the incident signal. The build-up time of the initial response and the persistence of the trailing oscillations are longest for a plasma with a critical electron density $\omega_p = \omega_s$, and increase with increasing distance from the source [3]. In an overdense plasma ($\omega_s/\omega_p = 0.5$), the main signal is cut off. Instead, weakly damped oscillations near the electron plasma frequency are excited at the beginning and at the end of the carrier pulse.

The excitation of the predicted transient oscillations and their decay in time have been observed experimentally by measuring the dispersion of short wave trains at a frequency of about 500 Mc/s in a neon afterglow plasma, confined in a coaxial transmission line 1.5 m long ($\theta \sim 15$). The apparatus is more fully described in Schmitt [1] and [2]. For the purposes of the present experiment, a phase-locked sinusoidal pulse with three cycles is generated by feeding a single three separate transmission lines. By adjustpulse with equal rise and fall times into three separate transmission lines. By adjusting the delay of each of the resultant pulses and recombining them in a single transmission line, a series of equally spaced pulses is obtained. The short RF pulse is generated by differentiating this pulse sequence by means of a small-series capacitor (approximately 2 pF in a 50-ohm transmission-line system).

In the absence of ionization, the coaxial line is approximately matched to the con-

Manuscript received March 10, 1965. The research reported in this correspondence was sponsored by the Air Force Cambridge Research Lab., Office of Aerospace Research, under Contract AF 19(628)-4183.